

Trajectory Optimization for Cellular-Enabled UAV with Connectivity and Battery Constraints

Hyeon-Seong Im, Kyu-Yeong Kim, and Si-Hyeon Lee

School of Electrical Engineering, Korea Advanced Institute of Science and Technology

Daejeon, South Korea

Emails: {imhyun1209, kimyou283, sihyeon}@kaist.ac.kr

Abstract—In this paper, we address the problem of path planning for a cellular-enabled UAV with connectivity and battery constraints. The UAV’s mission is to deliver a payload from an initial point to a final point, while maintaining connectivity with a BS and adhering to the battery constraint. The UAV’s battery can be replaced by a fully charged battery at a charging station, which takes some time. Our key contribution lies in proposing an algorithm that efficiently computes an optimal path that minimizes the mission completion time, solvable in polynomial time. We achieve this by transforming the problem into an equivalent two-level shortest path finding problem over weighted graphs and leveraging graph theoretic approaches to solve it. In more detail, we first find an optimal path and speed to travel between each pair of charging stations without replacing the battery, and then find the optimal order of visiting charging stations. To demonstrate the effectiveness of our approach, we compare it with previously proposed algorithms and show that our algorithm outperforms those in terms of both computational complexity and performance.

I. INTRODUCTION

Unmanned aerial vehicles (UAVs) are widely used in various scenarios, including cargo delivery [1], aerial surveillance [2], and flying base stations (BSs) [3]. Ensuring a continuous connection between the UAV and its control station is crucial for successful completion of the missions, but maintaining persistent communication becomes challenging when the UAV travels over long distances, due to factors such as large path loss and low line-of-sight probability [4], [5]. A promising solution to this problem is cellular-enabled UAV communication [6], wherein the BSs in the cellular network act as relays for communication. Therefore, finding a suitable trajectory for the UAV that enables efficient communication with a BS within the cellular network is of utmost importance.

Trajectory design problems for cellular-enabled UAVs have been extensively studied in various works [6]–[15]. In the work [6], the authors focused on optimizing the trajectory between an initial and a final location while maintaining communication with a base station (BS). They simplified the problem by assuming that the UAV could connect with a BS if the distance between them was less than a certain threshold. By doing so, they converted the problem into equivalent convex optimization and graph-theoretic shortest path finding problems and proposed one optimal (NP-hard) and two sub-optimal (NP-easy) algorithms. The study of characterizing

an optimal path has been extended in subsequent works to consider factors such as communication outage times [7], [8], 3D-building maps [9], radio map-based 3D path planning [10], and the collaboration of multiple UAVs [11]. In particular, the work [8] introduced the intersection method, which effectively reduces the time complexity by considering only the finite intersection points of the coverage boundaries of the BSs in path optimization. While these analytic approaches can derive an effective path for the UAV with low complexity, they might face challenges when dealing with scenarios with limited prior knowledge about the communication environment. In such cases, reinforcement learning (RL) [16] based approaches become effective, as they can approximate the communication environment empirically. The use of RL-based UAV path planning has been explored in several works [12]–[15]. However, it is important to note that the optimal path may not always be derived using the RL-based approach, and the training phase of RL can be time-consuming and resource-intensive.

In this paper, we address the problem of path planning for a cellular-enabled UAV, considering not only connectivity with a base station (BS) but also the UAV’s limited battery capacity. The scenario involves a cellular network with BSs and charging stations. The UAV’s mission is to deliver a payload from an initial point to a final point, while maintaining connectivity with a BS and adhering to the battery constraint. The UAV’s battery can be replaced by a fully charged battery at a charging station, but this process takes some time [17]. The primary challenge in this path planning problem is optimizing the route and the speed (since the energy consumption is affected by the speed) with the decisions about when and which charging station to visit. Our key contribution lies in proposing an algorithm that efficiently computes an optimal path for this problem, solvable in polynomial time (NP-easy). We achieve this by transforming the problem into an equivalent two-level shortest path finding problem over weighted graphs and leveraging graph theoretic approaches to solve it. More specifically, we first find an optimal path and speed to travel between each pair of charging stations without replacing the battery. Then, we find the optimal order of visiting charging stations to replace the battery. To demonstrate the effectiveness of our approach, we compare it with previously proposed algorithms in [6], [8] with slight modifications. The results show that our algorithm outperforms these existing approaches in terms of both computational complexity and performance.

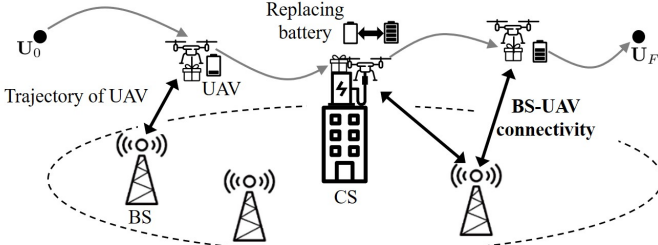


Fig. 1: An example of delivery and communication scenario of a UAV with three BSs and one CS. The UAV delivers a payload from \mathbf{U}_0 to \mathbf{U}_F under limited battery capacity while communicating with a BS. In the CS, the UAV can replace its battery.

II. PROBLEM STATEMENT

We consider a cellular network with M base stations (BSs) and $N \leq M$ charging stations (CSs). In this network, a UAV delivers a payload from an initial point \mathbf{U}_0 to a final point \mathbf{U}_F under limited battery capacity. The detailed description of the UAV model is in Section II-A. The UAV should maintain the connectivity with one of the BSs while delivering the payload. The BS model and the BS-UAV connectivity is described in Section II-B. The UAV can replace its battery at a CS if needed, as explained in Section II-C. The goal of this paper is to characterize the minimum delivery time from \mathbf{U}_0 to \mathbf{U}_F , including the flight time in the air and the battery swapping time at CSs. This optimization problem is formally presented in Section II-D. The overall model is illustrated in Fig. 1.

A. UAV Model

In the cellular network, a rotary-wing UAV has a mission of delivering a payload from an initial point \mathbf{U}_0 to a final point \mathbf{U}_F . We assume that the UAV flies with a fixed altitude $H \in [H_{\min}, H_{\max}]$, where H_{\min} is determined by the heights of obstacles in the network and H_{\max} corresponds to the maximum allowable altitude according to government regulations. Let us denote the 3D coordinates of \mathbf{U}_0 , \mathbf{U}_F , and the UAV location at time t by (x_0, y_0, H) , (x_F, y_F, H) , and $(x(t), y(t), H)$, respectively. We also denote $\mathbf{u}_0 = (x_0, y_0)$, $\mathbf{u}_F = (x_F, y_F)$, and $\mathbf{u}(t) = (x(t), y(t))$ as the horizontally projected locations of the 3D coordinates. The UAV flies with time-varying speed of $v(t) \triangleq \|\nabla_t \mathbf{u}(t)\|$ at time t , where the speed is selected from the finite set $\mathcal{V} = \{0, v_1, \dots, v_q\}$ with $0 < v_1 < \dots < v_q$.

For energy consumption, we only consider the propulsion energy consumption by the UAV, since the communication energy consumption is relatively negligible [3]. Let the total weight of UAV and its payload be given as $w = w_1 + w_2 + w_3$, where w_1 , w_2 , and w_3 denote the weights of the UAV body, its battery, and the payload, respectively. The propulsion power

consumption (in Watts) when flying with speed v is given as

$$P_{\text{UAV}}(v) = P_1 \left(1 + \frac{3v^2}{v_{\text{tip}}^2} \right) + P_2(w) \left(\sqrt{1 + \frac{v^4}{4v_0(w)^4}} - \frac{v^2}{2v_0(w)^2} \right)^{1/2} + \frac{\rho}{2} S_{\text{FP}} v^3, \quad (1)$$

where P_1 , $P_2(w)$, v_{tip} , $v_0(w)$, ρ , and S_{FP} are the parameters determined by the environment of the network and the physical structure of the UAV [18]. We note that the parameters $P_2(w)$ and $v_0(w)$ are only related to the total weight w . The power consumption model (1) and its parameters will be revisited with details in Section V.

The UAV consumes the remained energy in its battery. The battery capacity (in Joules) is expressed as follows [1]:

$$C_{\text{batt}} = \epsilon_{\text{batt}} w_2, \quad (2)$$

where ϵ_{batt} is the maximum energy of the battery per unit weight. Note that the battery capacity is directly proportional to the battery weight. As proved in [1], when the UAV flies at the same speed v without replacing its battery, then the maximum distance (in meters) that it can travel is given as

$$d_{\text{fly}}(v) = v \cdot \frac{\gamma \eta C_{\text{batt}}}{r_{\text{safe}} P_{\text{UAV}}(v)}, \quad (3)$$

where $0 < \gamma < 1$ is the maximum depth of discharge of the battery, $0 < \eta < 1$ is the power transfer efficiency from the battery to the UAV body, and $r_{\text{safe}} > 1$ is the safety factor to reserve energy in the battery for unexpected situations. We note that the consumed power in the battery is $\frac{r_{\text{safe}} P_{\text{UAV}}}{\gamma \eta}$, where the smaller γ and η and the larger r_{safe} reduce the energy consumption efficiency of the UAV.

B. BS-UAV Connectivity

There are M BSs in the cellular network. The m th BS where $m \in \mathcal{M} \triangleq [1 : M]$, BS_m is located at $(a_{m1}, a_{m2}, H_{\text{BS}})$, where all BSs are assumed to be located at the same altitude $H_{\text{BS}} < H$. We further denote $\mathbf{a}_m = (a_{m1}, a_{m2})$ as the horizontally projected location of BS_m . Each BS has a single omni-directional antenna and the same transmission power P_{tx} . All the BSs are connected to a control station through a backhaul network to successfully hand over from a BS to another BS and control the UAV trajectory.

We assume that the channel between the UAV and a BS is determined by the line-of-sight (LoS) probabilistic model, where the LoS probability increases as the elevation angle between the UAV and the BS increases [4]. The expected path loss between the UAV and BS_m at time t , $\Lambda_m(t)$ in dB is given as follows [5]:

$$\Lambda_m(t) = \text{FSPL}_m(t) + p_m(t) \cdot \zeta_1 + (1 - p_m(t)) \cdot \zeta_2, \quad (4)$$

where $\text{FSPL}_m(t)$ and $p_m(t) \in [0, 1]$ are the free space path loss and the LoS probability between the UAV and BS_m at time t , respectively, which only depend on the distance between the UAV and BS_m , and $\zeta_1 > 0$ and $\zeta_2 > \zeta_1$ refer to

the excessive path losses for LoS and non-LoS (NLoS) links, respectively.¹ The received signal to interference plus noise ratio (SINR) from BS_m to the UAV at time t is

$$\text{SINR}_m(t) = \frac{P_{\text{tx}} \cdot 10^{\Lambda_m(t)/10}}{\sum_{m' \in \mathcal{M} \setminus m} I_{m'm}(t) + N_0}, \quad (5)$$

where $I_{m'm}(t)$ is the interference power by BS_{m'} at time t when the UAV is communicating with BS_m and N_0 is the additive noise power. Note that $I_{m'm}$ would be equal to zero if BS_{m'} uses a different frequency band from BS_m, and even if the two BSs use the same frequency band, it will become negligible if BS_{m'} is far away from the UAV.

To maintain the control of the UAV, the communication rate from a BS to the UAV should not be less than the minimum required data rate, i.e., the maximally achievable SINR of the UAV should satisfy

$$\max_{m \in \mathcal{M}} \text{SINR}_m(t) \geq \text{SINR}_{\text{th}} \quad (6)$$

for any mission t where SINR_{th} is the hard SINR threshold to achieve the minimum required data rate. In weak interference regime, i.e., the frequency reuse factor is sufficiently low, it can be easily checked that the condition (6) can be equivalently written as $\min_{m \in \mathcal{M}} \|\mathbf{u}(t) - \mathbf{a}_m\| \leq d_0$ for some d_0 , where we call d_0 the base coverage radius of each BS.² For other cases, however, it is in general hard to represent the exact coverage region satisfying (6) in a simple form. For tractable analysis, we introduce the coverage offset $\lambda_m \in [0, d_0]$ for BS_m and assume that the UAV can connect with BS_m with high probability if the UAV is in the effective coverage region of BS_m given as $\|\mathbf{u}(t) - \mathbf{a}_m\| \leq d_0 - \lambda_m$.³ In other words, by introducing offsets λ_m taking into account the effect of interference, we assume that (6) holds with high probability if the following equation holds:

$$\min_{m \in \mathcal{M}} \|\mathbf{u}(t) - \mathbf{a}_m\| + \lambda_m \leq d_0. \quad (7)$$

Some examples of the effective coverage regions in the cellular network are illustrated in Fig. 2.

Remark 1. The possible coverage offset λ_m for $m \in \mathcal{M}$ depends on the environment around BS_m. For example, large (small) λ_m is appropriate for urban (suburban) environments since there are many (few) other BSs around BS_m. High flight altitude of BS_m induces large coverage offset λ_m since the interference from other BSs is easy to come to the LoS path [19]. Also, λ_m increases in the traffic of other BSs around BS_m since the received interference of the UAV is caused by the BSs which are not connected [10].

¹Our path loss model is based on large-scale fading, i.e., small-scale fading effects are ignored. However, we can check that our results also hold under the small-scale fading by averaging the randomness in it.

²Each BS has the same base coverage radius d_0 since every BS has the same transmission power P_{tx} and the same altitude H_{BS} , but it can be verified that our results also hold under different base coverage radii by different transmission powers or BS altitudes.

³In Section II-B, we only state the connectivity for the downlink communication from a BS to the UAV, but it can be checked that the similar coverage region as (6) is obtained in uplink communication scenarios.

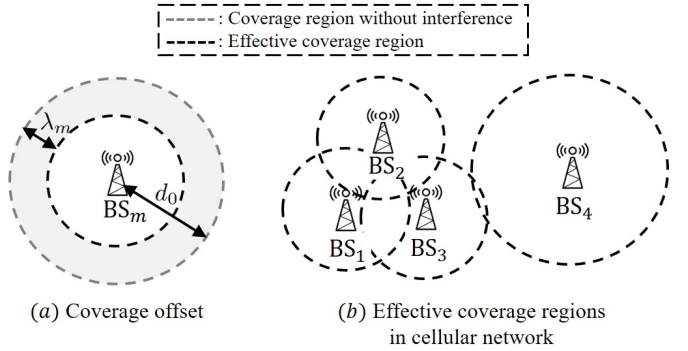


Fig. 2: Examples of effective coverage regions. (a) The coverage radius of BS_m is reduced by λ_m to account for the SINR reduction by interference. The shaded region may not be covered by BS_m. (b) Since BS₄ is isolated from the other BSs, $\lambda_4 < \lambda_i$ for $i \in [1 : 3]$.

C. Charging Station Model

To deliver the payload over a long distance with limited battery capacity, the UAV can replace its battery by visiting one of $N \leq M$ CSs. The n th charging station C_n where $n \in \mathcal{N} \triangleq [1 : N]$ is assumed to be located at $(c_{n1}, c_{n2}, H_{\text{CS}})$, where all CSs are assumed to be located at the same altitude $H_{\text{CS}} \leq H$. We further denote $\mathbf{c}_n = (c_{n1}, c_{n2})$ as the horizontally projected location of C_n . To reduce the delay to replace the battery, each CS uses the autonomous battery swapping system [17].⁴ The overall delay to replace the battery at charging station C_n , $\tau_{C_n} \in [0, \tau_{\text{max}}]$ consists of the waiting time and the battery swapping time, where τ_{max} is the upper bound on the delay. We note that the waiting time at charging station C_n varies depending on the congestion of the CS and hence τ_{C_n} depends on n .

Remark 2. When the UAV replaces the battery in a charging station C_n for $n \in \mathcal{N}$, there may be a loss due to battery swapping itself, as well as the overall delay τ_{C_n} to replace it. For example, the UAV may pay a fee to each visited CS. We can consider the loss by adding it to each τ_{C_n} .

D. Goal

The goal of this paper is to characterize the minimum delivery time T from \mathbf{U}_0 to \mathbf{U}_F of the UAV, including the flight time in the air and the overall delay to replace its battery at CSs. The optimization problem is formulated as

Problem 1

$$\text{Objective: } \min_{T \geq 0, \{\mathbf{u}(t), \psi(t), t \in [0, T]\}} T \quad (8)$$

Constraints:

$$\mathbf{u}(0) = \mathbf{u}_0, \mathbf{u}(T) = \mathbf{u}_F, E_{\text{batt}}(0) = C_{\text{batt}} \quad (9)$$

$$\mathbf{u}(t) \in \mathbb{R}^2, \psi(t) \in [0 : N] \quad (10)$$

$$v(t) \triangleq \|\nabla_t \mathbf{u}(t)\| \in \mathcal{V}, t \in [0, T] \quad (11)$$

⁴The autonomous battery swapping system in [17] takes about 60 seconds for the entire battery swapping process.

$$\min_{m \in \mathcal{M}} \|\mathbf{u}(t) - \mathbf{a}_m\| + \lambda_m \leq d_0, \quad t \in [0, T] \quad (12)$$

$$\psi(t) = 0 \text{ if } \mathbf{u}(t) \notin \{\mathbf{c}_n | n \in \mathcal{N}\}, \quad t \in [0, T] \quad (13)$$

$$\psi(t) \in \{0, n\} \text{ if } \mathbf{u}(t) \in \{\mathbf{c}_n | n \in \mathcal{N}\}, \quad t \in [0, T] \quad (14)$$

$$E_{\text{batt}}(t) \geq 0, \quad t \in [0, T] \quad (15)$$

$$\nabla_t E_{\text{batt}}(t) = -\frac{r_{\text{safe}}}{\gamma\eta} P_{\text{UAV}}(v(t)), \quad \psi(t) = 0, \quad t \in [0, T] \quad (16)$$

$$\nabla_t E_{\text{batt}}(t) = 0 \text{ if } \psi(t) \in \mathcal{N}, \quad t \in [0, T] \quad (17)$$

$$E_{\text{batt}}(t) = C_{\text{batt}} \text{ if } \psi(t) \in \mathcal{N} \text{ and}$$

$$t - \max_{t'} \{t' | \psi(t') = 0, t' \in [0, t]\} = \tau_{C_{\psi(t)}}, \quad t \in [0, T] \quad (18)$$

where $\psi(t) \in [0 : N]$ is an auxiliary variable indicating whether the UAV is in charging station C_n ($\psi(t) = n$) or in the air ($\psi(t) = 0$) at time t and $E_{\text{batt}}(t) \geq 0$ is the residual energy in the battery at time t . Here, (9) means that the UAV departs from \mathbf{u}_0 with fully charged battery and arrives at \mathbf{u}_F , (10) is the constraints for the optimized variables, (11) denotes that the UAV can fly with speed in \mathcal{V} , (12) is the connectivity constraint in (7), (13)-(14) determines whether the UAV is in a CS or in the air, (15) means that the remained energy in the battery should not have a negative value, (16) and (17) represent the power consumption when flying in the air and staying in a CS, respectively, and (18) means that the battery has the maximum energy when the battery swapping process is just finished.

Note that Problem 1 is not a convex optimization problem since the variable $\psi(t)$ is selected from a discrete set and constraint (12) is not convex. Moreover, $\mathbf{u}(t)$ should be optimized in continuous $t \in [0 : T]$. Such difficulties make Problem 1 non-trivial. To solve this problem, in Sections III and IV, we first reformulate Problem 1 in a framework of weighted graph and then show that the problem can be solved NP-easily by graph theory-based algorithms.

III. OPTIMAL TRAJECTORY WITH THE CONNECTIVITY CONSTRAINT

In this section, we provide an optimal solution for Problem 1 without the battery constraint, i.e., the battery capacity is assumed to be unlimited. We note that the UAV flies with the maximum speed v_q from \mathbf{U}_0 to \mathbf{U}_F since traveling with the maximum speed minimizes the mission time without the battery constraint. Such an optimization problem can be reformulated as follows:

Problem 1-1

$$\text{Objective: } \min_{T \geq 0, \{\mathbf{u}(t), t \in [0, T]\}} T \quad (19)$$

Constraints:

$$\mathbf{u}(0) = \mathbf{u}_0, \quad \mathbf{u}(T) = \mathbf{u}_F, \quad \mathbf{u}(t) \in \mathbb{R}^2 \quad (20)$$

$$\|\nabla_t \mathbf{u}(t)\| = v_q, \quad t \in [0, T] \quad (21)$$

$$\min_{m \in \mathcal{M}} \|\mathbf{u}(t) - \mathbf{a}_m\| + \lambda_m \leq d_0, \quad t \in [0, T] \quad (22)$$

Note that the optimization is still not trivial since it is non-convex and has an infinite number of variables.

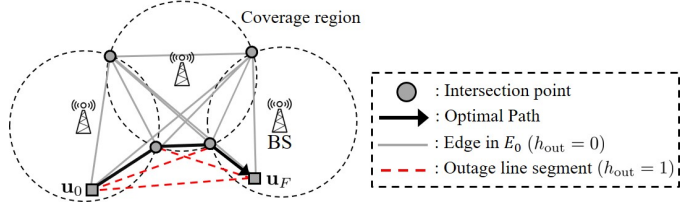


Fig. 3: An example of graph G_0 for $M = 3$. The graph has vertex set V_0 including \mathbf{u}_0 , \mathbf{u}_F , and all intersection points and edge set E_0 including the (solid) line segments between two vertices which lie inside the set of coverage regions.

To attack Problem 1-1, we propose a generalized intersection method that finds a trajectory of UAV satisfying the connectivity constraint by converting Problem 1-1 as an equivalent problem of finding the shortest path in an undirected weighted graph, and show that this generalized intersection method yields an optimal UAV path NP-easily. The pseudo code of the generalized intersection method is described in Algorithm 1. This algorithm first checks (in line 3) whether the problem is feasible or not via the checking feasibility function ChkFea , which outputs whether the problem 1-1 is feasible ($h_{\text{fea}} = 1$) or not ($h_{\text{fea}} = 0$) according to the initial point \mathbf{u}_0 , the final point \mathbf{u}_F , and the location and the effective coverage region of each BS. This function can be constructed by applying [6, Proposition 1] in the case that the BSs have the different coverage radii and its pesudo code is omitted. If the problem is feasible, an undirected weighted graph $G_0 = (V_0, E_0)$ is constructed based on the intersection points of the coverage boundaries (in lines 6-17). Specifically, the vertex set V_0 consists of the initial point \mathbf{u}_0 , the final point \mathbf{u}_F , and the intersection points of the coverage boundaries (in lines 6-10). The edge set E_0 is constructed (in lines 11-16) by including a line segment $\overline{\mathbf{x}_1 \mathbf{x}_2}$ between two different vertices $\mathbf{x}_1, \mathbf{x}_2 \in V_0$ if the line segment lies inside the set of coverage regions, which is checked through the function ChkOut whose pseudo code is provided in Algorithm 2 and is explained later. Such an edge is denoted by a tuple $(\mathbf{x}_1, \mathbf{x}_2, \|\mathbf{x}_1 - \mathbf{x}_2\|/v_q)$, where the weight of the edge $\|\mathbf{x}_1 - \mathbf{x}_2\|/v_q$ is given by the minimum travel time between \mathbf{x}_1 and \mathbf{x}_2 . After constructing a weighted undirected graph, an optimal path from \mathbf{u}_0 to \mathbf{u}_F over the graph is derived (in lines 18-19). We first find an optimal sequence \mathbf{S}_{V_0} of visiting nodes over the graph and the corresponding weight (equal to the mission time T) via the Dijkstra algorithm [20] that finds the minimum weight path between two nodes over a weighted graph with low complexity. Then, the corresponding UAV trajectory can be derived through the function FindPath , which outputs the UAV trajectory according to the sequence \mathbf{S}_{V_0} of visiting points and the speed v_q . This function can be constructed similarly as in [6, (25)-(27)] and its pseudo code is omitted. An example of the graph G_0 and the corresponding optimal trajectory by Algorithm 1 is illustrated in Fig. 3.

Algorithm 2 describes the function ChkOut which tests whether a line segment $\overline{\mathbf{x}_1 \mathbf{x}_2}$ between two different vertices

Algorithm 1 Generalized Intersection Method

Input: $v_q, \mathbf{u}_0, \mathbf{u}_F, \mathbf{a}_m, d_0, \lambda_m$ for $m \in \mathcal{M}$

1: **Def:** Function **ChkFea**($\mathbf{u}_0, \mathbf{u}_F, \mathbf{a}_m, d_0, \lambda_m$ for $m \in \mathcal{M}$) outputs whether Problem 1-1 is feasible ($h_{\text{fea}} = 1$) or not ($h_{\text{fea}} = 0$), where \mathbf{u}_0 is the initial point, \mathbf{u}_F is the final point, and d_0 and λ_m for $m \in \mathcal{M}$ are the parameters about the communication environment.

2: **Def:** Function **Dijkstra**($\mathbf{x}_1, \mathbf{x}_2, G$) for graph $G = (V, E)$ outputs (T, \mathbf{S}_V) , where T is the minimum total weight from $\mathbf{x}_1 \in V$ to $\mathbf{x}_2 \in V$ over the graph G and \mathbf{S}_V is the corresponding optimal sequence of visiting nodes in V .

3: $V_0 \leftarrow \{\mathbf{u}_0, \mathbf{u}_F\}, E_0 \leftarrow \emptyset$

4: $h_{\text{fea}} \leftarrow \text{ChkFea}(\mathbf{u}_0, \mathbf{u}_F, \mathbf{a}_m, d_0, \lambda_m$ for $m \in \mathcal{M}$)

5: **if** $h_{\text{fea}} = 1$ **then** \triangleright Problem 1-1 is feasible

▷ Step 1. Vertex construction: Construct a vertex set V_0 consisting of the initial, the final, and the intersection points.

6: **for** $m, m' \in \mathcal{M}, m < m'$ **do**

7: **if** $\|\mathbf{a}_m - \mathbf{a}_{m'}\| \leq 2d_0 - \lambda_m - \lambda_{m'}$ **then**

8: $V_0 \leftarrow V_0 \cup \{\mathbf{x} \in \mathbb{R}^2 \mid \|\mathbf{x} - \mathbf{a}_m\| = d_0 - \lambda_m, \|\mathbf{x} - \mathbf{a}_{m'}\| = d_0 - \lambda_{m'}\}$

9: **end if**

10: **end for**

▷ Step 2. Edge construction: Construct an edge set E_0 consisting of the line segments lying inside the set of coverage regions.

11: **for** $\mathbf{x}_1, \mathbf{x}_2 \in V_0, \mathbf{x}_1 \neq \mathbf{x}_2$ **do**

12: $h_{\text{out}} \leftarrow \text{ChkOut}(\mathbf{x}_1, \mathbf{x}_2, \mathbf{a}_m, d_0, \lambda_m$ for $m \in \mathcal{M}$)

13: **if** $h_{\text{out}} = 0$ **then**

14: $E_0 \leftarrow E_0 \cup (\mathbf{x}_1, \mathbf{x}_2, \|\mathbf{x}_1 - \mathbf{x}_2\|/v_q)$

15: **end if**

16: **end for**

▷ Step 3. Path search: Find an optimal path from the initial point to the final point over the graph.

17: $G_0 \leftarrow (V_0, E_0)$ \triangleright Construct graph G_0

18: $(T, \mathbf{S}_{V_0}) \leftarrow \text{Dijkstra}(\mathbf{u}_0, \mathbf{u}_F, G_0)$

19: $\mathbf{u}(t)$ for $t \in [0, T] \leftarrow \text{FindPath}(\mathbf{S}_{V_0}, v_q)$

20: **else** \triangleright Problem 1-1 is not feasible

21: $T \leftarrow \infty, \mathbf{u}(t) \leftarrow \text{Null}$ for $t \in [0, T]$

22: **end if**

Output: $h_{\text{fea}} \in \{0, 1\}, T, \mathbf{u}(t)$ for $t \in [0, T]$

$\mathbf{x}_1, \mathbf{x}_2 \in V_0$ lies in the set of coverage regions. We say that the line segment experiences an outage if there exists $\xi \in [0, 1]$ that satisfies the following condition:

$$\min_{m \in \mathcal{M}} \|\boldsymbol{\alpha}(\xi) - \mathbf{a}_m\| + \lambda_m > d_0, \quad (23)$$

where $\boldsymbol{\alpha}(\xi) \triangleq \mathbf{x}_1 + \xi(\mathbf{x}_2 - \mathbf{x}_1)$ for $\xi \in [0, 1]$ represents a point in the line segment $\overline{\mathbf{x}_1 \mathbf{x}_2}$. Here, (23) means that the UAV experiences an outage at point $\boldsymbol{\alpha}(\xi)$, i.e., the UAV cannot be connected with every BS at point $\boldsymbol{\alpha}(\xi)$. To check whether the line segment experiences an outage, the function **ChkOut** verifies whether there exists $\xi \in [0, 1]$ that satisfies (23). Let us define the safe interval $\mathcal{T}_{\text{safe}} \triangleq [0, \xi']$ for some $\xi' \in [0, 1]$

as the line segment such that every $\boldsymbol{\alpha}(\xi)$ for $\xi \in \mathcal{T}_{\text{safe}}$ has been checked to be inside the coverage regions, i.e., there exists $m \in \mathcal{M}$ such that $\|\boldsymbol{\alpha}(\xi) - \mathbf{a}_m\| + \lambda_m \leq d_0$. The function **ChkOut** first checks whether $\xi = 0$ is included in the coverage regions and then repeatedly updates the safe interval or declares an outage in the following way. Let the current safe interval be given as $[0, \xi'] \subseteq [0, 1]$. If the point $\boldsymbol{\alpha}(\xi' + \epsilon)$ is checked to be connected with BS_m for sufficiently small constant $\epsilon > 0$, then the safe interval is extended by including the range of ξ where $\boldsymbol{\alpha}(\xi)$ is connected with BS_m , i.e., $\|\boldsymbol{\alpha}(\xi) - \mathbf{a}_m\| \leq d_0 - \lambda_m$. This algorithm ends if $\boldsymbol{\alpha}(\xi' + \epsilon)$ cannot be connected with every BS ($h_{\text{out}} = 1$) or the safe interval reaches $[0, 1]$ ($h_{\text{out}} = 0$), where h_{out} is the indicator whether the line segment experiences an outage ($h_{\text{out}} = 1$) or not ($h_{\text{out}} = 0$). An example of updating the safe interval is shown in Fig. 4.

Algorithm 2 Function **ChkOut**

Input: $\mathbf{x}_1, \mathbf{x}_2 \in V_0, \mathbf{a}_m, d_0, \lambda_m$ for $m \in \mathcal{M}$

1: **Def:** $\boldsymbol{\alpha}(\xi) \triangleq \mathbf{x}_1 + \xi(\mathbf{x}_2 - \mathbf{x}_1)$ for $\xi \in [0, 1]$

2: $h_{\text{out}} \leftarrow 0, \xi' \leftarrow 0, \xi'' \leftarrow 0$

3: $\epsilon \leftarrow 10^{-10}$ \triangleright Sufficiently small positive constant

4: **while** $\xi' < 1$ **do**

▷ Update safe interval $\mathcal{T}_{\text{safe}}$ from $[0, \xi']$ to $[0, \xi'']$ if $\boldsymbol{\alpha}(\xi' + \epsilon)$ is included in the set of coverage regions.

5: **for** $m \in \mathcal{M}$ **do** \triangleright Find BS which covers $\boldsymbol{\alpha}(\xi' + \epsilon)$

6: **if** $\|\boldsymbol{\alpha}(\xi' + \epsilon) - \mathbf{a}_m\| \leq d_0 - \lambda_m$ **then**

7: $\xi'' \leftarrow \max\{\xi \in [0, 1] \mid \|\boldsymbol{\alpha}(\xi) - \mathbf{a}_m\| \leq d_0 - \lambda_m\}$

8: **break**

9: **end if**

10: **end for**

11: **if** $\xi'' = \xi'$ **then** $\triangleright \boldsymbol{\alpha}(\xi' + \epsilon)$ experiences an outage.

12: $h_{\text{out}} \leftarrow 1$

13: **break**

14: **end if**

15: $\xi' \leftarrow \xi''$

16: **end while** $\triangleright \xi' = 1$ means that $\mathcal{T}_{\text{safe}} = [0, 1]$.

Output: $h_{\text{out}} \in \{0, 1\}$

Now, the following theorems show that our generalized intersection method yields an optimal solution of Problem 1-1 NP-easily.⁵

Theorem 1. *The generalized intersection method outputs an optimal solution for Problem 1-1.*

Proof: We first notice that an optimal solution of Problem 1-1 consists of line segments, where its breakpoints are selected in the overlapping region of any two different BSs [6, Proposition 3] and the problem is equivalent to deriving a path which achieves the shortest distance from \mathbf{u}_0 to \mathbf{u}_F since the speed of the UAV is fixed at v_q . We prove the theorem by showing that an alternative solution whose breakpoints are only selected in the intersection points of the coverage

⁵We note that the intersection points are crucial for deriving an optimal trajectory as shown in Fig. 5.

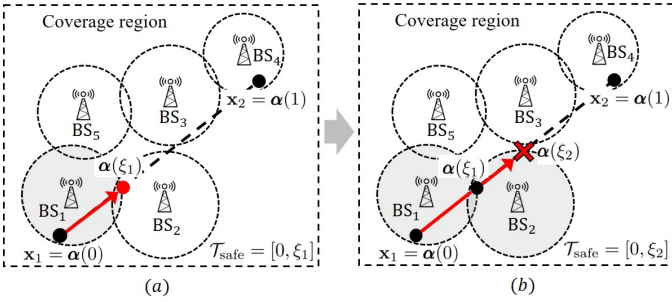


Fig. 4: An example of updating the safe interval T_{safe} in line segment $\overline{x_1x_2}$ for $M = 5$. (a) It first checks whether $\alpha(0)$ is connected with BS₁ and then refines the safe interval $T_{\text{safe}} = [0, \xi_1]$ by considering the coverage region of BS₁. (b) Since the UAV at $\alpha(\xi_1 + \epsilon)$ is connected with BS₂, the safe interval is updated to $T_{\text{safe}} = [0, \xi_2]$. Next, the UAV at $\alpha(\xi_2 + \epsilon)$ is not connected with every BS and hence $h_{\text{out}} = 1$.

boundaries can be always constructed and it achieves equal or smaller delivery time T compared to the solution of [6].

Without loss of generality, we consider a base trajectory with BS association sequence $[\text{BS}_1, \text{BS}_2, \dots, \text{BS}_k]$ for $k \leq M$, where its k 'th breakpoint $\beta_{k'} \in \mathbb{R}^2$ ($k' \leq k-1$) satisfies the following condition:

$$\|\beta_{k'} - \mathbf{a}_j\| \leq d_0 - \lambda_j \text{ for } j \in \{k', k' + 1\}. \quad (24)$$

For convenience, we set $\beta_k = \overline{\mathbf{u}_F}$. Such initial trajectory \mathcal{L} consists by the line segments $\overline{\mathbf{u}_0\beta_1}, \overline{\beta_1\beta_2}, \dots, \overline{\beta_{k-1}\beta_k}$. To reduce the length of the trajectory, we repeatedly update the trajectory \mathcal{L} from \mathbf{u}_0 to β_k . Let us define the completed path \mathcal{L}_c from \mathbf{u}_0 to $\overline{\mathbf{u}}$ is the completely updated part of the trajectory, where $\overline{\mathbf{u}} \in \mathbb{R}^2$ is the updating point. We repeatedly save the completely updated part of the trajectory \mathcal{L} in the completed path \mathcal{L}_c . We note that \mathcal{L}_c is updated by refining the updating point $\overline{\mathbf{u}}$ and its breakpoints are only selected in the intersection points. We start at the updating point $\overline{\mathbf{u}} \leftarrow \mathbf{u}_0$ and then verify whether $\overline{\mathbf{u}\beta_1}$ and $\overline{\beta_1\beta_2}$ can be replaced by $\overline{\mathbf{u}\beta_2}$ in the initial trajectory since $\|\overline{\mathbf{u}\beta_2}\| \leq \|\overline{\mathbf{u}\beta_1}\| + \|\overline{\beta_1\beta_2}\|$ holds by triangular inequality. If $\overline{\mathbf{u}\beta_2}$ does not experience an outage, then we update the initial trajectory as $\mathcal{L} : \overline{\mathbf{u}\beta_2}, \overline{\beta_2\beta_3}, \dots, \overline{\beta_{k-1}\beta_k}$ and repeat the same process until $\overline{\mathbf{u}\beta_i}$ ($i \in [2 : k]$) experiences an outage.⁶ When $\overline{\mathbf{u}\beta_i}$ experiences an outage, we have the updated trajectory $\mathcal{L} : \overline{\mathbf{u}\beta_{i-1}}, \overline{\beta_{i-1}\beta_i}, \dots, \overline{\beta_{k-1}\beta_k}$ satisfying the following inequality:

$$\|\overline{\mathbf{u}\beta_{i-1}}\| + \sum_{j=i}^k \|\overline{\beta_{j-1}\beta_j}\| \leq \ell_0, \quad (25)$$

where $\ell_0 = \|\overline{\mathbf{u}\beta_1}\| + \sum_{j=2}^k \|\overline{\beta_{j-1}\beta_j}\|$ is the length of the initial trajectory. Here, (25) means the length of the updated trajectory is not larger than ℓ_0 .

Next, we improve the trajectory $\mathcal{L} : \overline{\mathbf{u}\beta_{i-1}}, \overline{\beta_{i-1}\beta_i}, \dots, \overline{\beta_{k-1}\beta_k}$, where $i \in [2 : k]$ and $\overline{\mathbf{u}\beta_i}$ experiences an outage. Let

⁶We note that the trajectory $\overline{\mathbf{u}_0\mathbf{u}_F}$ is the alternative solution of Problem 1-1 if $\overline{\mathbf{u}_0\beta_k}$ does not still experience an outage.

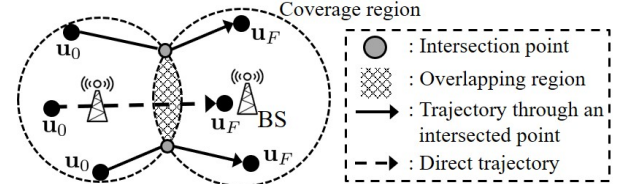


Fig. 5: An example of optimal trajectory for $M = 2$. The optimal trajectory for arbitrary \mathbf{u}_0 and \mathbf{u}_F is a (dashed) direct path or consists of two (solid) line segments through an intersection point.

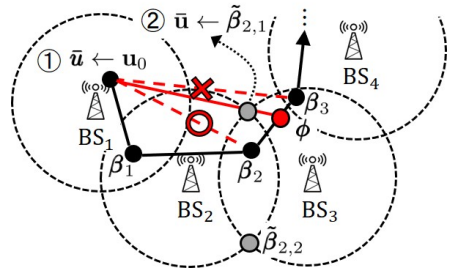


Fig. 6: An example of proof of Theorem 1. We first set the updating point $\overline{\mathbf{u}} \leftarrow \mathbf{u}_0$ and then verify that $\overline{\mathbf{u}\beta_2}$ does not experience an outage but $\overline{\mathbf{u}\beta_3}$ experiences an outage. Next, we update the trajectory $\mathcal{L} : \overline{\mathbf{u}\phi}, \overline{\phi\beta_3}, \dots$ and the updating point $\overline{\mathbf{u}} \leftarrow \overline{\beta_{2,1}}$.

us assume that $\tilde{\beta}_{i'1}$ and $\tilde{\beta}_{i'2}$ are the two intersection points of $\text{BS}_{i'}$ and $\text{BS}_{i'+1}$ where $i' \in [1 : k-1]$. We select a intersection point $\tilde{\beta}_{i',j}$ which satisfies the following condition:

$$\tilde{\beta}_{i',j} = \text{argmax}\{i' | \tilde{\beta}_{i',j} \in \Delta(\overline{\mathbf{u}\beta_{i-1}\beta_i}), \overline{\mathbf{u}\tilde{\beta}_{i',j}}$$

$$\tilde{\beta}_{i',j} \text{ lies in the set of the coverage regions}\}, \quad (26)$$

where $\Delta(\mathbf{x}_1\mathbf{x}_2\mathbf{x}_3)$ is the convex hull by $\mathbf{x}_1, \mathbf{x}_2, \mathbf{x}_3 \in \mathbb{R}^2$.⁷ Then, we can find the intersection $\phi \in \mathbb{R}^2$ of $\overline{\mathbf{u}\tilde{\beta}_{i',j}}$ and $\overline{\beta_{i-1}\beta_i}$. The trajectory \mathcal{T} is updated as $\overline{\mathbf{u}\phi}, \overline{\phi\beta_{i-1}}, \dots, \overline{\beta_{k-1}\beta_k}$ since the following holds by triangular inequality:

$$\|\overline{\mathbf{u}\phi}\| + \|\overline{\phi\beta_i}\| + \sum_{j=i+1}^k \|\overline{\beta_{j-1}\beta_j}\| \leq \ell_0. \quad (27)$$

Finally, we include the line segment $\overline{\mathbf{u}\tilde{\beta}_{i',j}} \subseteq \overline{\mathbf{u}\phi}$ as a part of the completed path \mathcal{L}_c and then refining the updating point $\overline{\mathbf{u}} \leftarrow \overline{\tilde{\beta}_{i',j}}$. We repeatedly perform the entire process at the remained trajectory $\overline{\mathbf{u}\phi}, \overline{\phi\beta_{i-1}}, \dots, \overline{\beta_{k-1}\beta_k}$ and update the completed path by refining $\overline{\mathbf{u}}$ until $\overline{\mathbf{u}\beta_k}$ does not experience an outage. The completed path \mathcal{L}_c from \mathbf{u}_0 to β_k including $\overline{\mathbf{u}\beta_k}$ is an alternative solution of Problem 1-1 since its length is not larger than ℓ_0 and it consists of the line segments whose breakpoints are in $\{\tilde{\beta}_{i,j} | i \in [1 : k-1], j \in \{1, 2\}\}$. The proof process is also shown in Fig. 6. ■

⁷It can be checked that the set in (26) is not an empty set.

Algorithm	Complexity	Performance gap
Exhaustive search [6]	$O(M!M^{3.5})$	0
Exhaustive search with fixed association [6]	$O(M^{3.5})$	$O(Md_0/v_q)$
Exhaustive search with quantization [6]	$O(M^4Q^2)$	$O((Md_0/v_q)\sin(1/Q))$
Intersection method [8] by checking outages via Algorithm 2	$O(M^4)$	$O(Md_0/v_q)$
Ours (Generalized intersection method)	$O(M^6)$	0

TABLE I: Comparison of algorithms for Problem 1-1

Theorem 2. *The time complexity of the generalized intersection method is $O(M^6)$.*

Proof: Let us first state the cardinality of the set $|V_0| = O(M^2)$. The steps in Algorithm 1 have the following complexities:

- Complexity of function ChkFea: It was shown that the complexity to check whether Problem 1-1 is feasible is $O(M^2)$ [6].
- Step 1. Vertex construction: This step has complexity $O(M^2)$ since the intersection points of the coverage boundaries by a BS pair is derived by calculating the quadratic equations in Line 6 of Algorithm 1 and the number of the possible BS pairs is $O(M^2)$.
- Step 2. Edge construction: The complexity of testing whether a line segment experiences an outage via the function ChkOut is $O(M^2)$ and every line segment $\overline{x_1x_2}$ by two different vertices $x_1, x_2 \in V_0$ should be tested. Hence, the complexity of this step is $O(M^2) \cdot |V_0|^2 = O(M^6)$.
- Step 3. Path search: The complexity of the Dijkstra algorithm in the graph G_0 is $O(|V_0|^2) = O(M^4)$ [21].

Consequently, the complexity of the generalized intersection method is $O(M^6)$, which is dominated at the edge E_0 construction step. ■

Now, let us compare our generalized intersection method with previously proposed algorithms to solve Problem 1-1. Table I summarizes the complexity and the performance gap from the optimal solution for each algorithm. In the following, we provide brief descriptions of previous algorithms and observations based on Table I.

- Among the algorithms in Table I, our generalized intersection method outputs an optimal solution NP-easily.
- The exhaustive search (ES), exhaustive search with fixed association (ES-FA), and exhaustive search with quantization (ES-Q) algorithms are proposed in [6]. In [6], it was shown that an optimal trajectory from u_0 to u_F consists of line segments, where its breakpoints are selected inside the overlapping regions of the coverage regions of two different BSs [6, Proposition 3]. In this approach, it is not possible to find an optimal solution via a graph theoretic approach since the overlapping regions consist of infinite number of points. The ES algorithm [6] is an optimal algorithm that finds optimal breakpoints inside the overlapping regions based on convex optimization, which is NP-hard over M . To reduce the complexity, two suboptimal algorithms are also proposed in [6], i.e., ES-

FA and ES-Q algorithms, which are NP-easy. The ES-FA algorithm is basically the same with ES algorithm, except that the sequence of BS association is fixed in advance, and the ES-Q algorithm applies a graph theoretic approach by quantizing each overlapping region to a finite number of the points. The ES-FA algorithm has lower complexity than the generalized intersection method, but its performance gap increases in M . For the ES-Q algorithm, let Q denote the number of quantization points in each overlapping region. Note that this algorithm has an increasing performance gap in M for $Q = O(M)$ and has a higher complexity than the generalized intersection method for $Q = \omega(M)$.

- The intersection method proposed in [8] only includes the intersection points as the possible breakpoints and applies a graph theoretic approach like our generalized intersection method. However, this algorithm is suboptimal because it searches a path for a fixed BS association sequence which is chosen in a heuristic way, similarly as the ES-FA algorithm [6]. Also, it does not explicitly suggest a function like our ChkOut function in Algorithm 2, checking whether each line segment between two vertices in the graph experiences an outage. If we apply the ChkOut function in Algorithm 2, the intersection method [8] has the same performance gap with the ES-FA algorithm [6] with a higher complexity.

IV. OPTIMAL TRAJECTORY WITH THE CONNECTIVITY AND BATTERY CONSTRAINTS

In this section, we target to solve Problem 1, i.e., optimize the UAV trajectory to minimize the mission time under the connectivity and the battery constraints.⁸ Note that it can be beneficial to change the UAV speed v under the battery constraint since the maximum travel distance without replacing the battery depends on v as shown in (3).

For Problem 1, we propose a generalized intersection method with battery constraint (GIM-B) by modifying our generalized intersection method in Section III, and show that this GIM-B algorithm outputs an optimal solution for Problem 1 NP-easily. The pseudo code for this GIM-B algorithm is provided in Algorithm 3. The resultant UAV trajectory from our algorithm consists of line segments between two points, where each point is one of the initial or final point, intersection points of the coverage boundaries, and CSs. The GIM-B algorithm determines the set of line segments (corresponding

⁸From now on, we assume that $H_{CS} = H$.

Algorithm 3 Generalized Intersection Method with Battery Constraint (GIM-B)

Input: $\mathbf{u}_0, \mathbf{u}_F, \mathbf{a}_m, d_0, \lambda_m, \mathcal{V}, \mathbf{c}_n, \tau_{C_n}, w, w_2$ for $m \in \mathcal{M}, n \in \mathcal{N}$

```

1: Def: Function BFS( $\mathbf{x}_1, \mathbf{x}_2, G$ ) for graph  $G = (V, E)$ 
   outputs 1 if  $\mathbf{x}_1 \in V$  and  $\mathbf{x}_2 \in V$  are connected in the
   graph  $G$  and otherwise outputs 0.
2:  $V_{\text{GL}} \leftarrow \{\mathbf{u}_0, \mathbf{u}_F, \mathbf{c}_1, \dots, \mathbf{c}_N\}, V_{\text{LO}}, E_{\text{LO}}, E_{\text{GO}} \leftarrow \emptyset$ 
3:  $V_{\text{in}}, E_{\text{in}}, E_1, \dots, E_{N+2} \leftarrow \emptyset$ 
    $\triangleright$  Consider the initial and the final points as CSs.
4:  $\mathbf{c}_{N+1} \leftarrow \mathbf{u}_0, \mathbf{c}_{N+2} \leftarrow \mathbf{u}_F, \tau_{C_{N+1}}, \tau_{C_{N+2}} \leftarrow 0$ 
5:  $V_{\text{in}} \leftarrow \text{All intersection points} \triangleright$  Lines 6-10 at Algorithm 1
6:  $V_{\text{all}} \leftarrow V_{\text{GL}} \cup V_{\text{in}}$ 
    $\triangleright$  Step 1. Outage test: Check whether each possible line
   segment experiences an outage.
7: for  $\mathbf{x}_1, \mathbf{x}_2 \in V_{\text{all}}, \mathbf{x}_1 \neq \mathbf{x}_2$  do
8:    $h_{\text{out}} \leftarrow \text{ChkOut}(\mathbf{x}_1, \mathbf{x}_2, \mathbf{a}_m, d_0, \lambda_m \text{ for } m \in \mathcal{M})$ 
9:   for  $n \in [1 : N + 2]$  do
10:    if  $h_{\text{out}} = 0, \mathbf{c}_n \in \{\mathbf{x}_1, \mathbf{x}_2\}$  then
11:       $E_n \leftarrow E_n \cup (\mathbf{x}_1, \mathbf{x}_2, \|\mathbf{x}_1 - \mathbf{x}_2\|)$ 
12:    end if
13:   end for
14:   if  $h_{\text{out}} = 0, \mathbf{c}_n \notin \{\mathbf{x}_1, \mathbf{x}_2\}$  for  $n \in [1 : N + 2]$  then
15:      $E_{\text{in}} \leftarrow E_{\text{in}} \cup (\mathbf{x}_1, \mathbf{x}_2, \|\mathbf{x}_1 - \mathbf{x}_2\|)$ 
16:   end if
17: end for
    $\triangleright$  Step 2. Local level search: Derive optimal paths between
   each pair of CSs.
18: for  $n \in [1 : N + 1], n' \in [1 : N] \cup \{N + 2\}, n \neq n'$  do
    $\triangleright$  Function ChkFea is described in line 1 at Algorithm 1.
19:    $h_{\text{Lfea}} \leftarrow \text{ChkFea}(\mathbf{c}_n, \mathbf{c}_{n'}, \mathbf{a}_m, d_0, \lambda_m \text{ for } m \in \mathcal{M})$ 
20:   if  $h_{\text{Lfea}} = 1$  then
21:      $V_{\text{LO}} \leftarrow V_{\text{in}} \cup \{\mathbf{c}_n, \mathbf{c}_{n'}\}, E_{\text{LO}} \leftarrow E_{\text{in}} \cup E_n \cup E_{n'}$ 
22:      $G_{\text{LO}} \leftarrow (V_{\text{LO}}, E_{\text{LO}})$ 
    $\triangleright$  Function Dijkstra is described in line 2 at Algorithm 1.
23:      $(\ell_{\text{LO}}, \mathbf{S}_{V_{\text{LO}}}(\mathbf{c}_n, \mathbf{c}_{n'})) \leftarrow \text{Dijkstra}(\mathbf{c}_n, \mathbf{c}_{n'}, G_{\text{LO}})$ 
24:      $(h_{\text{sp}}, v(\mathbf{c}_n, \mathbf{c}_{n'})) \leftarrow \text{ChkSp}(\ell_{\text{LO}}, \mathcal{V}, w, w_2)$ 
25:     if  $h_{\text{sp}} = 1$  then
26:        $E_{\text{GL}} \leftarrow E_{\text{GL}} \cup (\mathbf{c}_n, \mathbf{c}_{n'}, \ell_{\text{LO}}/v(\mathbf{c}_n, \mathbf{c}_{n'}) + \tau_{C_{n'}})$ 
27:     end if
28:   end if
29: end for
    $\triangleright$  Step 3. Global level search: Derive an optimal path from
   the initial point to the final point over the graph of CSs.
30:  $\vec{G}_{\text{GL}} \leftarrow (V_{\text{GL}}, E_{\text{GL}}) \quad \triangleright \vec{G}_{\text{GL}}$  is a directed graph.
31:  $h_{\text{Gfea}} \leftarrow \text{BFS}(\mathbf{u}_0, \mathbf{u}_F, \vec{G}_{\text{GL}})$ 
32: if  $h_{\text{Gfea}} = 1$  then
33:    $(T, \mathbf{S}_{V_{\text{GL}}}(\mathbf{u}_0, \mathbf{u}_F)) \leftarrow \text{Dijkstra}(\mathbf{u}_0, \mathbf{u}_F, \vec{G}_{\text{GL}})$ 
34:    $(\mathbf{u}(t), \psi(t) \text{ for } t \in [0, T]) \leftarrow \text{FindPathG}(\mathbf{S}_{V_{\text{GL}}},$ 
       $v(\mathbf{c}_n, \mathbf{c}_{n'}), \mathbf{S}_{V_{\text{LO}}}(\mathbf{c}_n, \mathbf{c}_{n'}), \tau_{C_{n'}} \text{ for } n \in [1 : N + 1],$ 
       $n' \in [1 : N] \cup \{N + 2\})$ 
35: else
36:    $h_{\text{Gfea}} \leftarrow 0, T \leftarrow \infty, \mathbf{u}(t), \psi(t) \leftarrow \text{Null} \text{ for } t \in [0, T]$ 
37: end if

```

Output: $h_{\text{Gfea}} \in \{0, 1\}, T, \mathbf{u}(t), \psi(t) \text{ for } t \in [0, T]$

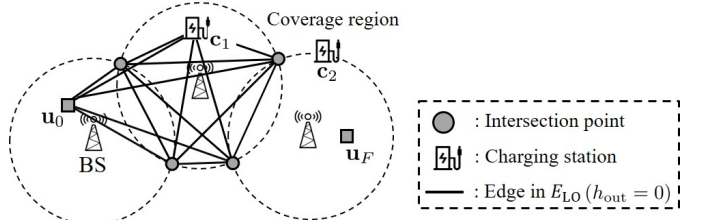


Fig. 7: An example of graph $G_{\text{LO}} = (V_{\text{LO}}, E_{\text{LO}})$ in the local level of Algorithm 3, where $M = 3$ and $N = 2$.

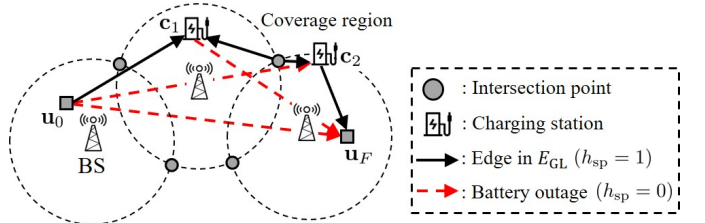


Fig. 8: An example of graph $\vec{G}_{\text{GL}} = (V_{\text{GL}}, E_{\text{GL}})$ in the global level of Algorithm 3, where $M = 3$ and $N = 2$.

to edges in the equivalent graphs) that are connected one after another in three steps. First, it checks whether each possible line segment experiences an outage and constitutes the no-outage edge sets (in lines 7-17). Then, the algorithm finds the optimal path in two levels. In the local level (in lines 18-29), it finds the optimal path between each pair of CSs (by treating the initial and the final points also as CSs) by applying Dijkstra algorithm and derives the maximum allowable speed to travel between each pair of CSs by applying the function ChkSP whose pseudo code is in Algorithm 4.⁹ In this local level, note that it may not be possible to travel between two CSs because there is no path between them ($h_{\text{Lfea}} = 0$) or because the distance is too large to travel with the battery capacity ($h_{\text{sp}} = 0$). An example of the graph to derive an optimal path between two CSs at the local level is illustrated in Fig. 7. In the global level (in lines 30-35), we consider a directed graph whose vertex set consists of CSs and edge set consists of edges between CSs which has been checked to be reachable in the local level, with the weights of traveling and battery swapping time. For this graph, the algorithm first checks whether it is feasible to travel from the initial to the final points via the function breadth-first search (BFS) [21], which searches all connected nodes from a start node in a graph with low complexity. If feasible, it constructs the UAV trajectory by applying the Dijkstra algorithm over the graph and then applying the function FindPathG that outputs the trajectory based on the sequence of visiting points in the global and the local levels, the speeds traveling between CSs, and the battery swapping times. An example of the graph to derive an optimal path between from the initial point to the final point at the global level is illustrated in Fig. 8.

Algorithm 4 describes the function ChkSp which checks

⁹We assume that the UAV flies with a fixed speed while traveling through a path at the local level, which is justified later in Theorem 3.

whether the UAV can travel a distance $\ell_{\text{LO}} \geq 0$ without replacing the battery ($h_{\text{sp}} = 1$) or not ($h_{\text{sp}} = 0$) by using the maximum possible traveling distance function $d_{\text{fly}}(v)$ in (3) for speed $v \in \mathcal{V}$. If it is possible ($h_{\text{sp}} = 1$), then it derives the maximum possible speed $v_{\text{max}} \in \mathcal{V}$ whose maximum traveling distance $d_{\text{fly}}(v_{\text{max}})$ is not smaller than ℓ_{LO} . We note that the algorithm assumes that the UAV flies with a fixed speed between two CSs, while the speed can vary depending on the pair of CSs. The following theorem shows a sufficient condition for flying with a fixed speed between two CSs to be optimal.

Algorithm 4 Function ChkSp

Input: ℓ_{LO} , \mathcal{V} , w , w_2

- 1: **if** $\{v \in \mathcal{V} | d_{\text{fly}}(v) \geq \ell_{\text{LO}}\} \neq \emptyset$ **then**
- 2: $h_{\text{sp}} \leftarrow 1$ \triangleright Can travel ℓ_{LO} without battery swapping
 \triangleright Find the maximum possible speed v_{max} that can travel the length ℓ_{LO} without battery swapping.
- 3: $v_{\text{max}} \leftarrow \max_{v \in \mathcal{V}} \{v | d_{\text{fly}}(v) \geq \ell_{\text{LO}}\}$
- 4: **else**
- 5: $h_{\text{sp}} \leftarrow 0$, $v_{\text{max}} = 0$
- 6: **end if**

Output: $(h_{\text{sp}}, v_{\text{max}})$

Theorem 3. *Assume that the UAV can fly with any speed $v \in [v_1, v_q]$ and the power consumption model $P_{\text{UAV}}(v)$ is convex for $v \in [v_1, v_q]$. Then, for traveling between two CSs with the connectivity and battery constraints, flying with a fixed speed minimizes the traveling time.*

Proof: Let us assume that the path distance ℓ_{LO} to travel between two CSs is partitioned by segments ℓ_1, \dots, ℓ_K where $\ell_{\text{LO}} = \sum_{k=1}^K \ell_k$ and the UAV flies with speed $\tilde{v}_k \in [v_1, v_q]$ for segment ℓ_k for $k \in [1 : K]$. In this case, we have the total travel time $T_{\text{LO}} = \sum_{k=1}^K \ell_k / \tilde{v}_k$ and the total consumed energy $E_{\text{LO}} = \sum_{k=1}^K (\ell_k / \tilde{v}_k) \cdot P_{\text{UAV}}(\tilde{v}_k)$. We prove this theorem by showing the UAV can travel ℓ_{LO} within time T_{LO} by a fixed speed $\bar{v} \in [v_1, v_q]$ while consuming less energy than E_{LO} . First, the UAV can travel ℓ_{LO} in time T_{LO} if it travels with the fixed speed $\bar{v} = \frac{\ell_{\text{LO}}}{\sum_{k'=1}^K \ell_{k'} / \tilde{v}_{k'}}$. Second, E_{LO} is lower-bounded as:

$$E_{\text{LO}} = \sum_{k=1}^K (\ell_k / \tilde{v}_k) \cdot P_{\text{UAV}}(\tilde{v}_k) \quad (28)$$

$$\stackrel{(a)}{\geq} \left(\sum_{k'=1}^K \ell_{k'} / \tilde{v}_{k'} \right) \cdot P_{\text{UAV}} \left(\sum_{k=1}^K \frac{\ell_k / \tilde{v}_k}{\sum_{k'=1}^K \ell_{k'} / \tilde{v}_{k'}} \cdot \tilde{v}_k \right) \quad (29)$$

$$= T_{\text{LO}} \cdot P_{\text{UAV}}(\bar{v}), \quad (30)$$

where (a) is by Jensen's inequality. Since the UAV with fixed speed \bar{v} consumes less energy than E_{LO} as (30), this proves the theorem. \blacksquare

We note that the power consumption model in (1) can be approximated as a convex function when $v \gg v_0(w)$ as proved

in [18].¹⁰ Hence, in Algorithm 1, traveling with a fixed speed between two CSs, while the speed can vary depending on the pair of CSs, is approximately optimal.

Now, the following theorems show that our GIM-B algorithm outputs an optimal solution of Problem 1 NP-easily under the assumption that the power consumption model $P_{\text{UAV}}(v)$ is convex in the range of the UAV speed.¹¹

Theorem 4. *The GIM-B algorithm outputs an optimal solution for Problem 1 if the power consumption model $P_{\text{UAV}}(v)$ is convex in the range of the UAV speed.*

Proof: This proof is immediate from Theorems 1 and 3 and the optimality of the Dijkstra algorithm because

- 1) Theorem 1 means that every path between two CSs at the local level has the minimum travel distance.
- 2) Theorem 3 implies that flying with the same speed in each path at the local level is optimal. Hence, the GIM-B algorithm derives the minimum travel time for the paths.
- 3) Under the graph \vec{G}_{GL} with the minimized edge weights, an optimal trajectory from \mathbf{u}_0 to \mathbf{u}_F at the global level is derived by applying the Dijkstra algorithm. \blacksquare

Theorem 5. *If the number of CSs is smaller than or equal to the number of BSs, i.e., $N \leq M$, then the time complexity of the GIM-B algorithm is $O(M^6)$.*

Proof: Let us first state the cardinalities of the following sets: $|V_{\text{all}}| = O(M^2)$, $|V_{\text{LO}}| = O(M^2)$, and $|V_{\text{GL}}| = O(N)$. The steps of Algorithm 3 have the following complexities:

- Step 1. Outage test: For a line segment, performing the function ChkOut and selecting a memory to save the line segment among $E_{\text{in}}, E_1, \dots, E_{N+2}$ have the complexities $O(M^2)$ and $O(N)$, respectively. Since each line segment $\overline{\mathbf{x}_1 \mathbf{x}_2}$ for $\mathbf{x}_1, \mathbf{x}_2 \in V_{\text{all}}$ and $\mathbf{x}_1 \neq \mathbf{x}_2$ should be checked whether experiencing an outage, the complexity of this step is $(O(M^2) + O(N)) \cdot |V_{\text{all}}|^2 = O(M^6)$.
- Step 2. Local level search: The complexity of deriving an optimal path between a pair of CSs at the local level can be proved similarly with the proof of Theorem 2. However, this algorithm constructs the edge set E_{LO} with only complexity $O(N)$ by just loading some of the saved memories $E_{\text{in}}, E_1, \dots, E_{N+2}$. Hence, the complexity of deriving an optimal path in the local level is $O(N) + O(M^4) = O(M^4)$. Since there are $O(N^2)$ pairs of the CSs, the complexity of the step is $O(M^4 N^2)$.
- Step 3. Global level search: This complexity is dominated by applying the Dijkstra algorithm at the graph \vec{G}_{GL} with the complexity $O(|V_{\text{GL}}|^2) = O(N^2)$ [21].

Consequently, the complexity of the GIM-B algorithm is $O(M^6)$ for $N \leq M$. \blacksquare

¹⁰Such convexity of the power consumption model $P_{\text{UAV}}(v)$ will be numerically shown in Section V.

¹¹We assume $|\mathcal{V}| = O(M)$ to make the complexity of selecting v_{max} in Algorithm 4 negligible.

Algorithm (*modified considering the battery constraint)	Complexity	Performance gap
Exhaustive search* [6]	$O(M!M^{3.5}N^2)$	0
Exhaustive search with fixed association* [6]	$O(M^{3.5}N^2)$	$O(MNd_0/v_q + N\tau_{\max})$
Exhaustive search with quantization* [6]	$O(M^4Q^2N^2)$	$O(MNd_0/v_q + N\tau_{\max})$
Intersection method* [8] by checking outages via Algorithm 2	$O(M^4N^2)$	$O(MNd_0/v_q + N\tau_{\max})$
Ours (Generalized intersection method with battery constraint)	$O(M^6)$	0

TABLE II: Comparison of algorithms for Problem 1

We note that our GIM-B algorithm has the same complexity order as the generalized intersection method for $N \leq M$ despite considering the battery constraint. Note that the outage of every possible line segment is tested in advance in Step 1 of GIM-B algorithm. However, a direct extension from the GIM algorithm would be treating the pair of CSs as the initial and final points and applying a modified version of Algorithm 1, which implies performing the outage test in Step 2. The following corollary shows that such a direct extension of the GIM algorithm has a higher order of complexity.

Corollary 1. *If the outage test is separately performed in the derivation of an optimal path between each pair of CSs, the time complexity increases to $O(M^6N^2)$.*

Proof: This method checks whether each line segment experiences an outage at the step 2 in Algorithm 3. In this case, the complexity for deriving a path between two CSs at the local level through the step 2 is the same as the complexity $O(M^6)$ of the generalized intersection method. Hence, the complexity of this method is dominated at deriving $O(N^2)$ paths for every CS pair: $O(M^6) \cdot O(N^2) = O(M^6N^2)$. ■

Table II compares the GIM-B algorithm with the benchmark algorithms for Problem 1. We note that the benchmark algorithms in Table II use the same name as Table I but they are modified by considering the battery constraint. Specifically, we modify each benchmark algorithm similarly as Algorithm 3: Step 1 is skipped since it is not applicable for the exhaustive search and its variants [6] and it is not beneficial for the intersection method [8], Step 2 applies the corresponding benchmark algorithm with slight modification by treating the two CSs as the initial and the final points and checking whether traveling the resultant path is affordable with the battery capacity, and Step 3 applies the Dijkstra algorithm to obtain the trajectory in the global level. To compare with the results in Table I, we assume that the UAV flies with a constant speed of v_q for the analysis of performance gap in Table II, i.e., assume $\mathcal{V} = \{0, v_q\}$. Also, to avoid the meaningless bound of infinite gap, it is assumed that a path from the initial point to the final point exists in Step 3 for each algorithm, i.e., assume $h_{\text{Gfea}} = 1$. Main observations for Table II are summarized in the following:

- The GIM-B algorithm outputs an optimal solution of Problem 1 NP-easily.
- The performance gaps of the sub-optimal algorithms increase in N due to the accumulation of the gaps in finding the path between each pair of CSs. Also, note that they

depend on the maximum delay τ_{\max} for battery swapping because the number of visiting CSs can increase for the sub-optimal algorithms.

- Compared to Table I, the performance gap of the ES-Q algorithm with the finite number Q of quantization points does not decrease in Q , because some of the edges in the graph \vec{G}_{GL} over the CSs of the GIM-B algorithm may disappear if we apply ES-Q algorithm in Step 2 due to the battery constraint.

The aforementioned analysis implies that our intersection point-based algorithms have more advantages compared to the benchmark algorithms in the presence of the battery constraint and the CSs.

Remark 3. *When $H_{\text{CS}} < H$, we can solve Problem 1 by including the take-off and the landing times at charging station C_n in overall delay τ_{C_n} for $n \in \mathcal{N}$ and considering the consumed energy for them in the battery capacity model (2).*

Remark 4. *If we do not take any assumptions in Table II, then the performance gaps of the sub-optimal algorithms increase compared to this table. First, when we assume that the UAV flies with dynamic speed (i.e., $|\mathcal{V}| \geq 3$ where $0 \in \mathcal{V}$), the maximum possible speed v_{\max} in a path between two CSs at the local level decreases as its distance ℓ_{LO} increases. Hence, it should be considered in the performance gaps that when the distance ℓ_{LO} increases, its travel time additionally increases due to decreasing v_{\max} . Second, a path from the initial point to the final point may not exist in Step 3 for some sub-optimal algorithms (i.e., $h_{\text{Gfea}} = 0$) since some of the edges in the graph \vec{G}_{GL} over the CSs of the GIM-B algorithm may disappear if we apply the sub-optimal algorithms in Step 2 due to the battery constraint.*

V. NUMERICAL RESULTS

In this section, we provide various numerical results to evaluate the performance of our GIM-B algorithm. We assume that $M = 19$ BSs and $N = 5$ CSs are distributed in a $10\text{km} \times 10\text{km}$ region where \mathbf{u}_0 and \mathbf{u}_F are located. The coverage radius of BS_m is set with $d_0 = 1400\text{m}$ and $\lambda_m \in [0, 700]\text{m}$ for $m \in \mathcal{M}$. The overall delay to replace the battery at charging station C_n is assumed to be $\tau_{C_n} = 100\text{s}$ for $n \in \mathcal{N}$. The speed set of the UAV is $\mathcal{V} = [0 : 1 : 30]\text{m/s}$. The total weight of the UAV including its payload is given as $w = 2.97\text{kg}$, where $w_1 = 1.07\text{kg}$, $w_2 = 0.9\text{kg}$, and $w_3 = 1\text{kg}$. The detailed parameters for the propulsion power consumption (1) are set to $P_1 = 42.24\text{J}$, $P_2(w) = 445.19\text{J}$, tip speed of the blade $v_{\text{tip}} = 14\text{m/s}$, mean rotor induced speed for

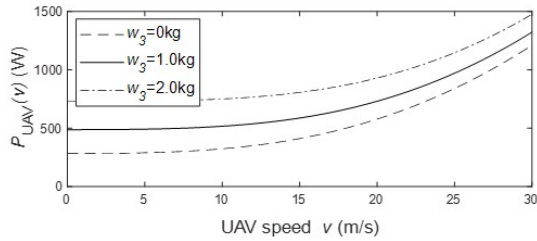


Fig. 9: Propulsion power consumption (1) versus speed v for different payload weights w_3 .

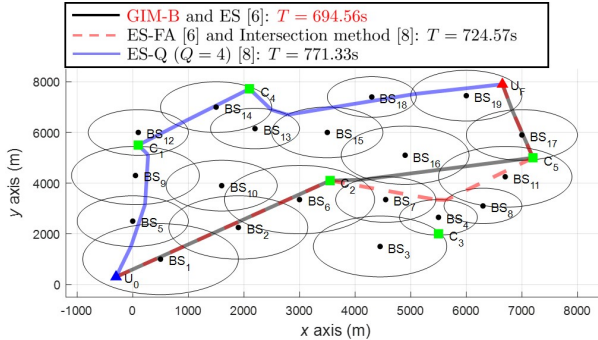


Fig. 10: Comparison of trajectory and the corresponding delivery time T for algorithms to solve Problem 1.

hovering $v_0(w) = 13.9\text{m/s}$, air density $\rho = 1.225\text{kg/m}^3$, and fuselage equivalent flat plate area $S_{\text{FP}} = 0.03\text{m}^2$. Also, the battery model (2)-(3) is assumed to have the parameters $\epsilon_{\text{batt}} = 540\text{kJ/kg}$, $\gamma = 0.7$, $\eta = 0.7$, and $r_{\text{safe}} = 1.2$ [1].¹² Fig. 9 plots the propulsion power consumption $P_{\text{UAV}}(v)$ according to the flying speed v in different payload weights w_3 , where we can numerically check that $P_{\text{UAV}}(v)$ is a convex function for $v \in [0, 30]\text{m/s}$ and hence the conditions in Theorems 3 and 4 hold.

Fig. 10 shows the UAV trajectory and the corresponding delivery time T for our and benchmark algorithms. We note that the ES-FA algorithm [6] and intersection method [8] find the same trajectory, but different from the optimal trajectory of the ES algorithm [6] and our GIM-B algorithm. The ES-Q algorithm [6] with $Q = 2$ cannot find any trajectory from \mathbf{u}_0 to \mathbf{u}_F due to the battery constraint. The ES-Q algorithm with $Q = 4$ has a higher complexity than our GIM-B algorithm because $QN > M$. However, it has a significant lower travel time T even than the ES-FA and the intersection method algorithms, since it cannot derive a path \mathbf{u}_0 to \mathbf{c}_2 with the quantization points that the UAV can travel without battery replacement. Fig. 11 shows the optimal graph at the global level and the corresponding maximum possible speed v_{max} for each edge under the environment in Fig. 10. We can see that for each edge, the maximum travel speed v_{max} decreases as its travel distance increases.

Fig. 12 compares the optimal UAV trajectory and the corresponding delivery time T for the different payload weights w_3 and delays τ_{C_1} to replace the battery at charging station

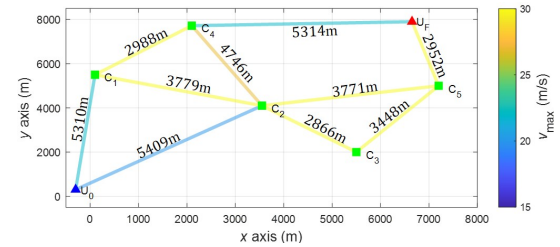


Fig. 11: Optimal graph at the global level and the corresponding maximum possible speed v_{max} for each edge.

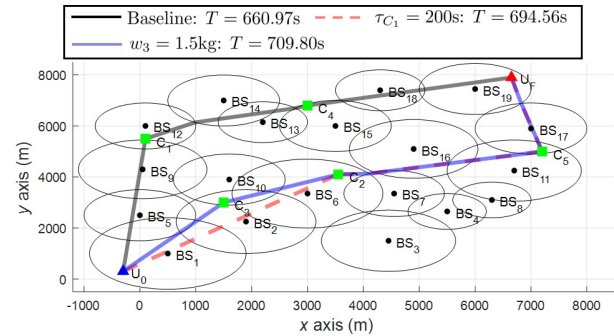


Fig. 12: Comparison of optimal trajectory and the corresponding delivery time T for the case that battery swapping delay $\tau_{C_1} = 200\text{s}$ and payload weight $w_3 = 1.5\text{kg}$.

C_1 , where the locations of CSs C_3 and C_4 are changed from Fig. 10. We can see that the UAV avoids C_1 in high battery swapping delay $\tau_{C_1} = 200\text{s}$ (red) and visits more CSs in large payload weight $w_3 = 1.5\text{kg}$ (blue). In Fig. 13, the optimal delivery time T is plotted for the different battery swapping delays and the payload weights $w_3 \in [0 : 0.1 : 3.5]\text{kg}$ under the environment in Fig. 12. We can verify that T increases as battery swapping delays and w_3 increase and the payload cannot be delivered from \mathbf{u}_0 to \mathbf{u}_F if w_3 exceeds 2.8kg .

VI. CONCLUSION

For the problem of path planning for a cellular-enabled UAV with connectivity and battery constraints, the generalized intersection method with battery constraint (GIM-B) algorithm was proposed that computes an optimal path in polynomial time. Its effectiveness in terms of computational complexity and resultant mission completion time was demonstrated

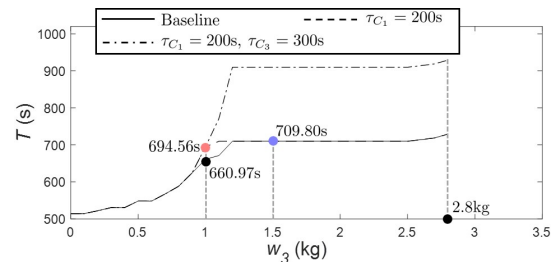


Fig. 13: Payload weight w_3 versus optimal delivery time T for different τ_{C_1} and τ_{C_3} .

¹²We note that the values of $P_2(w)$ and $v_0(w)$ depend on w as [18].

by comparing with previously proposed algorithms both in analytically and numerically. For further works, it would be interesting to consider the scenario with time-varying delays at charging stations and the scenario with more realistic coverage regions based on radio map.

REFERENCES

- [1] J. Zhang, J. F. Campbell, D. C. Sweeney II, and A. C. Hupman, "Energy consumption models for delivery drones: A comparison and assessment," in *Transportation Research Part D: Transport and Environment*, vol. 90, 2021, p. 102668.
- [2] K. Kanistras, G. Martins, M. J. Rutherford, and K. P. Valavanis, "A survey of UAVs for traffic monitoring," in *2013 International Conference on Unmanned Aircraft Systems*, 2013, pp. 221–234.
- [3] M. Mozaffari, W. Saad, M. Bennis, Y.-H. Nam, and M. Debbah, "A tutorial on UAVs for wireless networks: Applications, challenges, and open problems," in *IEEE Communications Surveys and Tutorials*, vol. 21, no. 3, 2019, pp. 2334–2360.
- [4] A. Al-Hourani, S. Kandeepan, and S. Lardner, "Optimal LAP altitude for maximum coverage," in *IEEE Wireless Communications Letters*, vol. 3, no. 6, 2014, pp. 569–572.
- [5] A. Al-Hourani, S. Kandeepan, and A. Jamalipour, "Modeling air-to-ground path loss for low altitude platforms in urban environments," in *2014 IEEE Global Communications Conference*, 2014, pp. 2898–2904.
- [6] S. Zhang, Y. Zeng, and R. Zhang, "Cellular-enabled UAV communication: A connectivity-constrained trajectory optimization perspective," in *IEEE Transactions on Communications*, vol. 67, no. 3, 2019, pp. 2580–2604.
- [7] S. Zhang and R. Zhang, "Trajectory design for cellular-connected UAV under outage duration constraint," in *2019 IEEE International Conference on Communications*, 2019, pp. 1–6.
- [8] Y.-J. Chen and D.-Y. Huang, "Trajectory optimization for cellular-enabled UAV with connectivity outage constraint," in *IEEE Access*, vol. 8, 2020, pp. 29 205–29 218.
- [9] O. Esrafilian, R. Gangula, and D. Gesbert, "3D-map assisted UAV trajectory design under cellular connectivity constraints," in *2020 IEEE International Conference on Communications*, 2020, pp. 1–6.
- [10] S. Zhang and R. Zhang, "Radio map-based 3D path planning for cellular-connected UAV," in *IEEE Transactions on Wireless Communications*, vol. 20, no. 3, 2021, pp. 1975–1989.
- [11] A. Chapnevius, s. Güvenç, L. Njilla, and E. Bulut, "Collaborative trajectory optimization for outage-aware cellular-enabled UAVs," in *2021 IEEE 93rd Vehicular Technology Conference*, 2021, pp. 1–6.
- [12] Y. Zeng and X. Xu, "Path design for cellular-connected UAV with reinforcement learning," in *2019 IEEE Global Communications Conference*, 2019, pp. 1–6.
- [13] Y. Zeng, X. Xu, S. Jin, and R. Zhang, "Simultaneous navigation and radio mapping for cellular-connected UAV with deep reinforcement learning," in *IEEE Transactions on Wireless Communications*, vol. 20, no. 7, 2021, pp. 4205–4220.
- [14] Y.-J. Chen and D.-Y. Huang, "Joint trajectory design and BS association for cellular-connected UAV: An imitation-augmented deep reinforcement learning approach," in *IEEE Internet of Things Journal*, vol. 9, no. 4, 2022, pp. 2843–2858.
- [15] X. Wang and M. C. Gursoy, "Learning-based UAV trajectory optimization with collision avoidance and connectivity constraints," in *IEEE Transactions on Wireless Communications*, vol. 21, no. 6, 2022, pp. 4350–4363.
- [16] R. S. Sutton and A. G. Barto, *Reinforcement learning: An introduction*. Cambridge, MA, USA: A Bradford Book, 2018, vol. 2.
- [17] D. Lee, J. Zhou, and W. T. Lin, "Autonomous battery swapping system for quadcopter," in *2015 International Conference on Unmanned Aircraft Systems*, 2015, pp. 118–124.
- [18] Y. Zeng, J. Xu, and R. Zhang, "Energy minimization for wireless communication with rotary-wing UAV," in *IEEE Transactions on Wireless Communications*, vol. 18, no. 4, 2019, pp. 2329–2345.
- [19] X. Lin *et al.*, "Mobile network-connected drones: Field trials, simulations, and design insights," in *IEEE Vehicular Technology Magazine*, vol. 14, no. 3, 2019, pp. 115–125.
- [20] E. W. Dijkstra, "A note on two problems in connexion with graphs." in *Numerische Mathematik*, vol. 1, 1959, pp. 269–271.
- [21] D. B. West, *Introduction to graph theory*. New Jersey, USA: Prentice Hall, 2001, vol. 2.